Numerical study of light backscattering from layers of absorbing irregular particles larger than the wavelength

Samer Alhaddad[1], Jens Förstner[1], Yevgen Grynko[1]

[a]*Department of Theoretical Electrical Engineering, Paderborn University, Warburger Str. 100, Paderborn, 33098, , Germany*

Abstract

We simulate light backscattering from monolayers of absorbing irregular particles larger than the wavelength using a numerically exact discontinuous Galerkin time domain (DGTD) method. Varying the real and imaginary parts of the complex refractive index m, particle size and the structure of a monolayer we study the evolution of the negative polarization (NP) feature that is observed for many particulate surfaces near backscattering. Simulations show that the NP is enhanced when increasing absorption from $Im(m)$=0.06 to 0.3. The real part $Re(m)$ plays little role in this case. We confirm correlation of NP with the particle size predicted by approximate models and observed in laboratory measurements. We also demonstrate that the interplay between single- and multiple scattering can be controlled by the topography of a monolayer resulting in enhanced or damped NP.

Keywords: light scattering, polarization, polarimetry
PACS: 42.68.Mj

1.

Optical remote sensing of natural powder-like surfaces is a tool that allows characterization of remote objects through photopolarimetric observations. It is used in the monitoring the surface of the Earth, studying the Moon and the Solar System bodies that scatter solar light [1, 2, 3]. The surfaces of planetary sattelites, asteroids and cometary nuclei are usually covered with debris material called regolith which is formed by meteoroid bombardment of primordial compositionally heterogeneous objects. As a result, regolith consists of dust, broken rocks and glasses. The abundant materials that are found on the surfaces different types of bodies at different distances from the

Sun are Fe- and Mg-rich silicates, carbonaceous materials, feldspars, calcite and organic compounds [4, 5] . The icy bodies in the Kuiper Belt objects as well as polar regions on Earth are covered with ice particles [6]. This covers a broad range of refractive indices and absorption properties. As a result of space weathering, the regolith particles have irregular shapes and different sizes which range from subwavelength scales to hundreds of microns (e.g., [7]).

Photopolarimetric measurements can be used for solving the inverse problem of the physical parameter retrieval for such surfaces. Using observational data one can estimate particle size, refractive index of the material, packing density and analyze surface topography [1, 2, 3, 8, 9, 10, 11]. If other kind of data like reflectance spectra, multi-wavelength polarimetry at backscattering and intermediate phase angles, thermal inertia measurements, etc., is available one can further constrain the physical properties of the surface of the target object.

The Solar System objects are often observed near backscattering and, therefore, backscattering phenomena are of interest in this case. They are intensity enhancement and negative polarization (NP) [1, 3, 12, 13, 14]. Intensity often shows strong angular dependence governed by shadowing effect [3] due to the increasing shadow area with decreasing scattering angle. The dependence can become nonlinear within a few degrees near exact backscattering [15]. Such an intensity surge (IS) results from the weak localization of light in a discrete disordered medium [16]. In linear polarization, the so-called negative polarization (NP) branch is a common feature observed for many kinds of fine powders. Initially unpolarized, solar radiaton scattered from a disordered surface obtains a non-zero polarization degree. It can be defined as $P = \frac{I_\perp - I_\parallel}{I_\perp + I_\parallel}$, where $I_\perp$ and $I_\parallel$ are intensities measured at the perpendicular and parallel orientations of the analyzer with respect to the scattering plane. NP at backscattering from particulate media may have different sources depending on the particle size and absorption [17, 18, 19, 3, 20, 21, 22]. Non-absorbing particles can reveal a strong NP feature in a wide range of sizes [23, 24]. Diffuse multiple scattering component can only suppress their contribution to the total scattering decreasing the degree of negative polarization [25] while the inversion angle remains unchanged.

At high absorption light scattering from interior of single particles larger than the wavelength can not be a source of NP, however, dark low-albedo powders may produce a comparable NP feature (e.g., [13]). In this case one

should involve double and, possibly, higher-order scattering into consideration. Indeed, approximate models of coherent backscattering that take into account interference of the scattered fields in pairs of scatterers can explain the phenomenon [17, 18, 19, 26]. We also validated this mechanism in a realistic model of layers of densely packed irregular particles recently [21, 27].

Large variation of the particles sizes and absorption properties imply variation of single scattering albedos of particles that form natural surfaces in a wide range. Correspondingly, this makes an impact on the light transport regime and mean transport length of propagation in a particulate medium that depends on absorption. The imaginary part of the complex refractive index of the material can be nearly zero, have transient or large values leading to dark surfaces with geometric albedos as low as a few percents (e.g., [10]). There can be also mixtures of absorbing and non-absorbing particles. Thus, the solution of the inverse problem for each particular case requires understanding of the mechanisms of light propagation in such media. This implies significant efforts in numerical modelling as analytical theories and approximate models often can not provide a clear explanation of the observed phenomena unless they are validated and compared with the results of numerically exact simulations [28] and experimental measurements (e.g., [29]). The main problems here are the multi-scale geometry of fine powders as a class of discrete media and the complex mechanism of near-field interaction between particles that becomes important at packing densities $\rho > 0.1$ [20, 21]).

In this work we continue the study of backscattering from layers of densely packed absorbing irregular particles using numerical simulations. We reveal the roles of the complex refractive index, particle size and topography of the surface formed by a particulate layer that they play in the formation of the backscattering phenomena and negative polarization, in particular.

2. Model description

We apply a full wave approach and use the discontinuous Galerkin time domain method (DGTD) [30] to solve the electromagnetic problem of light scattering. We consider isolated Gaussian random field (GRF) particles [31, 32] and monolayers with finite dimensions formed by such particles. The constituents are randomly oriented and have the size parameters $kR = 20$ and $kR = 30$, where k is the wave-number and R is the radius of the circumscribing sphere. For this numerical study we do not consider size distributions

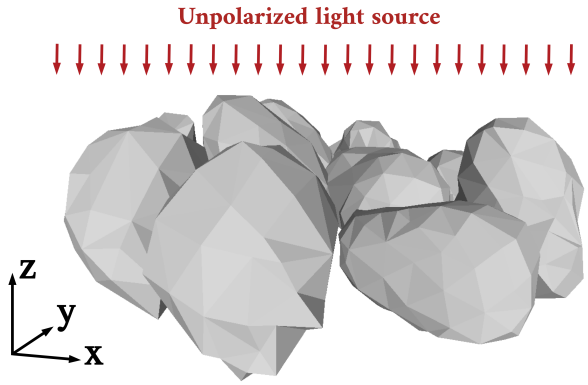

Figure 1: A monolayer sample with ten densely packed compact irregular particles.

and take these sizes as they are characteristic for many natural powders (e.g., [33]) and laboratory powder samples being larger than the wavelength. An example of the model structure of ten densely packed particles mimicking the geometry of a powder-like surface is shown in Fig. 1. We use the Bullet physics engine [34] to create such clusters with minimum distance between irregular constituents much smaller than the wavelength. This is an open-source C++ library that simulates dynamics and collisions of arbitrary 3d objects in time domain. For thick plane layers of tens [21] and spherical clusters of thousands of such particles [25], generated with the same parameters, the packing density is estimated as large as $\rho \approx 0.5$. The number of constituents N = 10 for all samples is chosen as a result of the study of backscattering from absorbing monolayers of different sizes. In Ref. [21] we considered structures with up to 100 particles. The relative contribution of single scattering from the sample edges with particle size $kR \sim 30$ becomes insignificant starting from $N \sim 10$ which provides a converging solution for scattering angles $120 - 180^\circ$ [21, 27].

We consider three values of the real part of refractive index $Re(m) = 1.3$, 1.5, and 1.8. The imaginary part values are $Im(m) = 0.06$, which represents an absorbing dielectric, and $Im(m) = 0.1$ and $Im(m) = 0.3$, which can be characterized as transient materials. Generally, such values of m are characteristic for iron-rich silicates or carbonaceous materials (e.g., [35, 36]). In this work we study the properties of NP as a result of only multiple scattering and, therefore, we do not consider lower absorption regimes $Im(m) <$ 0.06 where single scattering NP emerge. A similar problem has been studied

previously (e.g., [37, 38, 39]) but systems of much smaller sizes and smaller constituents were considered.

In our model an unpolarized a plane wave source illuminates a monolayer sample at normal incidence (Fig. 1) with a pulse duration providing a steady state of the resulting near field. For the purpose of simulating an infinite domain preventing unwanted artificial reflections from the boundaries, perfectly matched layers (PML) are used. The numerical solution is represented by the scattered near field amplitudes that are transformed to far-field quantities from which then the scattering Mueller matrix elements as functions of the scattering angle are obtained [40]. As we deal with ensembles of random irregular shapes and randomly structured monolayers all the presented curves are averaged over 100 to 300 samples. This number depends on the convergence rate of the result in each particular case. Single compact absorbing particles are relatively simple scatterers, therefore, quickly converging intensity and polarization require 100-200 samples. Multiple scattering in monolayers slows convergence down and the number of ~ 300 samples is needed.

3. Results and discussion

Here we present the results of numerical simulations of light scattering by absorbing single particles and monolayers consisting of them. Varying parameters of the complex refractive index, size and surface topography we study the changes in intensity and linear polarization curves near backscattering.

3.1. The complex refractive index effect

In this section we study the effect of absorption of the material concentrating on the mechanism of formation of NP at backscattering. The results of simulations for single GRF particles and monolayers are shown in Fig. 2. The intensity curves for single particles in Figs. 2a and 2c are normalized by the integral intensity of scattering in all directions by single non-absorbing particles (conservative case) of the same set which corresponds to the total energy incident on the geometric cross-section and relates such a ratio to the Bond albedo. This relation is, however, not direct as diffraction must be excluded according to the definition of the Bond albedo [41]. The geometric single-scattering albedo can be estimated by comparison of the backscattering intensities in the conservative and absorbing cases. Fig. 2a shows that

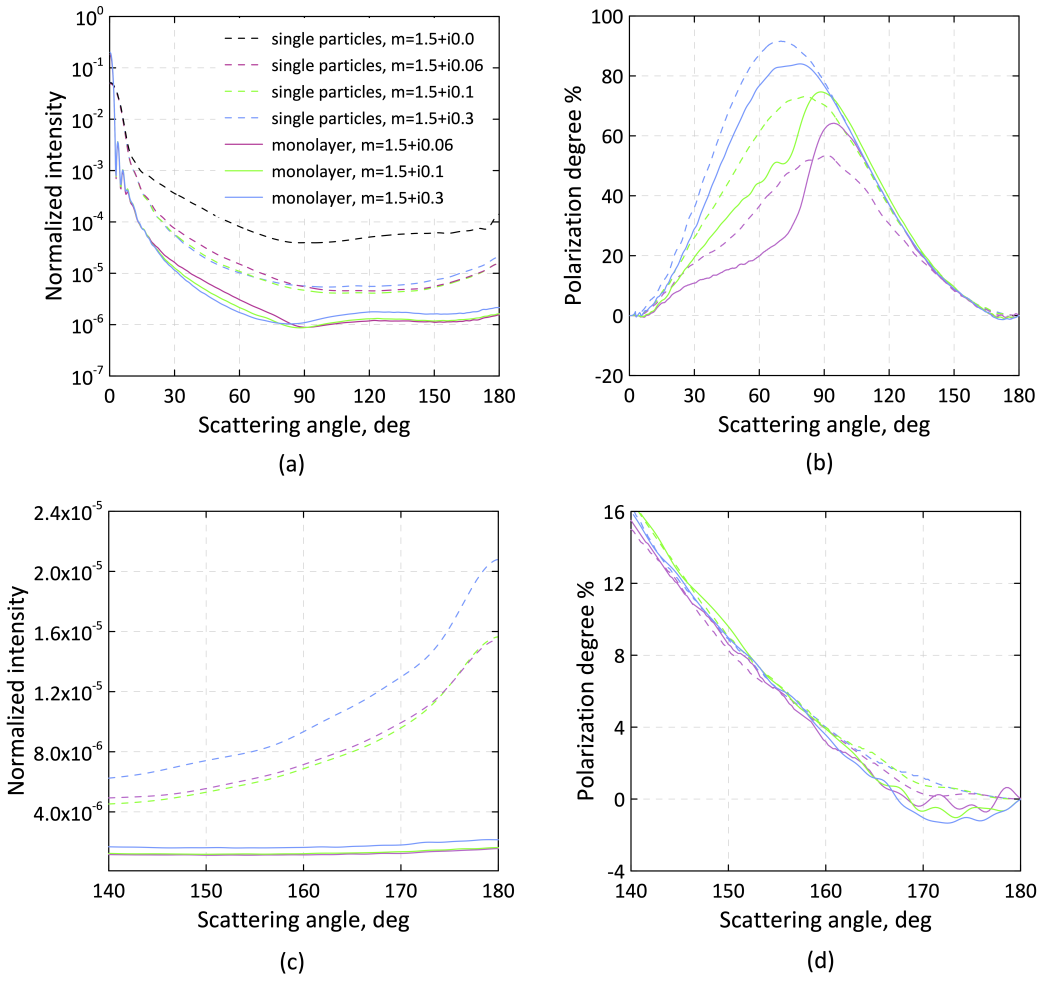

Figure 2: Scattering angle dependencies of the normalized intensity in logarithmic (a) and linear (c) scale and degree of linear polarization (b), (d) computed for single GRF particles with size parameter $kR = 30$ and monolayers of 10 particles with different imaginary parts of the complex refractive index ($Im(m) = 0.06$, 0.1, and 0.3).

it is smaller than at least 10%. Increasing scattering in the backward hemisphere with absorption is a consequence of the increasing external reflection coefficient at large $Im(m)$. We note also that single particles are relatively more efficient at backscattering than monolayers and show steeper intensity curves at large scattering angles (Fig. 2c). The degree of linear polarization for single scattering by such particles shows an expected behavior. Increasing $Im(m)$ we obtain a higher linear polarization maximum due to absorption of

the internal scattering component and growing relative contribution of external reflection. At $Im(m) = 0.3$ the positive maximum reaches almost 100% which is a high value usually not observed in laboratory measurements. Our model particles are larger than the wavelength and have relatively smooth surface, therefore, scattering is represented mostly by Fresnel-like external reflection. This property explains also the effect we study below.

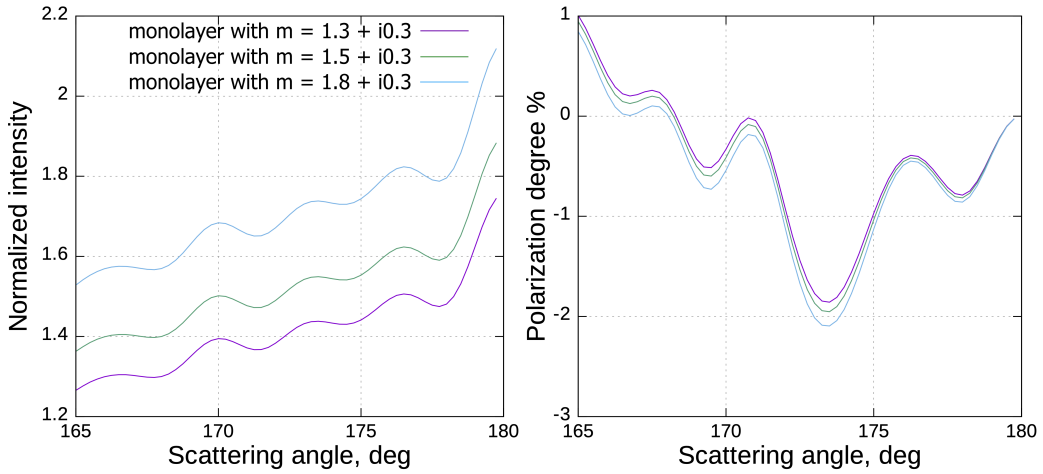

(a) (b)

Figure 3: Scattering angle dependencies of the normalized intensity (a) and degree of linear polarization (b) computed for monolayers of 10 absorbing GRF particles with different real parts of the complex refractive index ($Re(m) = 1.3$, 1.5 and 1.8). The size parameter of constituents is $kR = 30$.

Single scattering does not produce NP at all three values of $Im(m)$. The single-particle polarization curve for $Im(m) = 0.06$ in Fig. 2d goes along zero level in the range of 170-180°. This is a transient case. Below this value internal scattering in single particles becomes strong enough to produce NP which we want to avoid in our study. Hence, the NP feature that is present for monolayers (Fig. 2d) is a result of multiple scattering between close neighbor constituents.

The enhancement of NP in Fig. 2d acn be explained. Scattering orders higher that 2 are unlikely to contribute significantly to backscattering from a dense system of absorbing particles larger than the wavelength. At the same time analytical models of coherent backscattering [18, 19, 17] considering second order scattering supported by numerical simulations [21, 22] explain the origin of NP well enough. Thus, we conclude that the NP in Fig. 2d is

an interference effect in second order scattering that interplays with the first order external reflection.

The demonstrated dependence of NP on absorption can be taken into account in the analysis of the polarimetric data obtained for low albedo asteroids and surfaces of other Solar System objects as one of the factors influencing the depth of the NP branch. To summarize, we can recall the backscattering NP as a single-scattering property of non-absorbing and low-absorbing particles. It dampens with increasing absorption and disappears at some value of $Im(m)$ depending on the particle size. In a multi-particle system it re-appears as result of coherent backscattering from pairs of neighbor constituents. Thus, in a wide range of $Im(m)$ from 0.0 to $\sim$0.3 the evolution of the NP parameters can be complicated and non-monotonous which makes the solution of the retrieval problem more difficult and requires further systematic studies.

We note also, that single particles produce a pronounced backscattering intensity surge (Fig. 2c). Therefore, the IS for absorbing monolayers can be a result of single scattering contribution and coherent backscattering enhancement produced by second and higher orders.

A similar but weaker effect in polarization is observed if we vary the real part of the complex refractive index. The results obtained for three values of $Re(m)$ are compared in Fig. 3. For all three cases the same set of 100 samples was used. We limited the number of samples as the effect of $Re(m)$ became clear after 100 simulations. The resonance oscillations can be smoothed out with larger number but the small difference between the polarization curves will be retained. Increasing $Re(m)$ changes the external reflection coefficient and we see a weak enhancement of NP as Fig. 3b shows. Such a small difference can be detected in observations, however, it is too small for reliable analysis and determination of $Re(m)$ for multi-disperse powders consisting absorbing particles larger than the wavelength.

3.2. The role of particle size and surface topography

The structure of the monolayers in our model creates conditions for coherent backscattering. Therefore, one can expect that the size of constituent particles plays a role here and changes in the polarization curve can be detected. At dense packing different sizes produce different topographies in monolayers changing the interference bases for counter-propagating waves. Such an effect is predicted by analytical models [18, 19, 17] and is also observed in the laboratory measurements of size separated absorbing samples

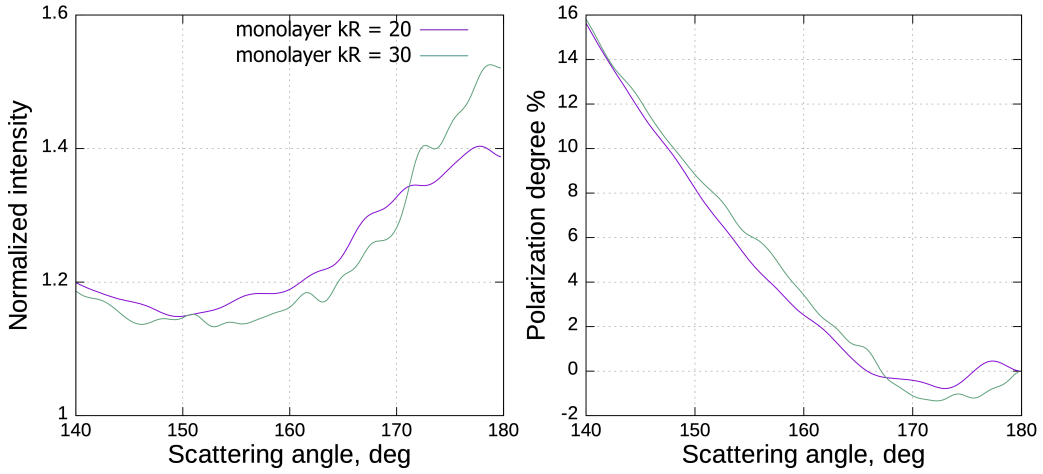

(a) (b)

Figure 4: Scattering angle dependencies of the normalized intensity (a) and degree of linear polarization (b) computed for monolayers of 10 GRF particles with size parameters of constituents $kR = 20$ and $kR = 30$. The complex refractive index is $m = 1.5 + i0.3$.

[13]. In Fig. 4 we compare intensity and polarization curves computed for monolayers with sizes of constituent particles kR=20 and kR=30. Despite the size difference is not very large one can see the size effect in intensity Fig. 4a and polarization Fig. 4b. It is broadening of the backscattering features, both IS and NP, for smaller constituents and, correspondingly, finer structure of the layer surface. Thus, we confirm the prediction of approximate models with a more realistic particulate structure.

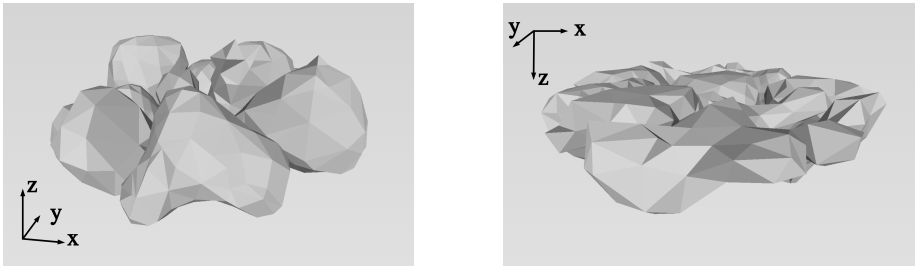

(a) Top view of sample 1 (b) Bottom view of sample 1

Figure 5: Top and bottom views of the same monolayer sample showing difference in topography.

In the last figure we show an interesting effect of vanishing NP feature in

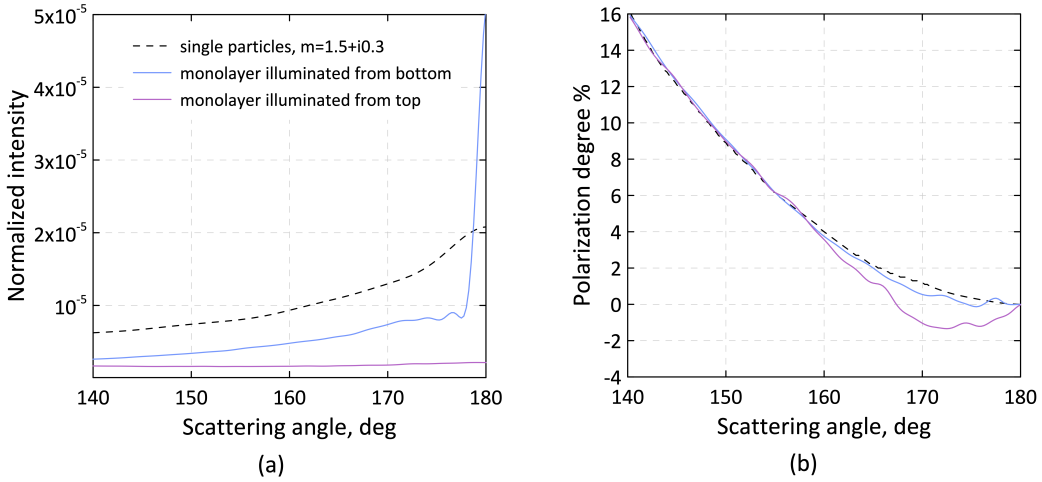

Figure 6: Scattering angle dependencies of the normalized intensity (a) and degree of linear polarization (b) computed for single particles and monolayers of 10 particles with $kR = 30$ illuminated from top and bottom at m $= 1.5 + i0.3$.

a dense monolayer of particles with the size $kR = 30$ and complex refractive index m $= 1.5 + i0.3$. The preparation of samples includes simulations of the free fall of particles on a substrate with dynamic interactions until a steady state. As a result we obtain a random topography of the upper side of monolayers (Fig. 5a). The bottom side is different. It is formed by random particles with their largest plane areas (Fig. 5b). This is an effect of multiple collisions with the substrate and random rotations. Another important property is that these plane elements are located at the same level perpendicular to the direction of incidence of light. As a result, we can see an increasing backscattering intensity and a specular reflection peak in Fig. 6a. In polarization such an increase of single scattering contribution results in the absence of NP (Fig. 6b) although it is still a dense particulate monolayer consisting of the same number of irregular particles. The relative area of corner-like topological forms, where NP originates from, becomes too small and coherent backscattering can not counteract the single scattering component that is positively polarized.

With this we can specify geometrical factors that influence the strength of the NP effect at high absorption. Generally, this is an interplay of the particle size and particle packing density in the very upper layer that determine relative contributions of single and double scattering. Low packing density, i.e. large distance between constituents (of any size) results in dom-

inating single scattering and little NP effect [22]. Close packing increases the possibility for double scattering and interference of counter-propagating waves and enhancement of NP. At maximum density a particle size effect can be clearly seen in polarization. Smaller particles create a finely structured surface with smaller interference bases which increases the inversion angle. Larger particles create larger corner-like shapes between them and, correspondingly narrower and deeper NP.

4. Conclusion

We study monolayers of absorbing irregular particles larger than the wavelength and focus on the evolution of the NP feature near backscattering varying with the complex refractive index and monolayer geometry. Our simulations show that NP caused by coherent backscattering gets enhanced with increasing absorption from $Im(m)$=0.06 to 0.3. Single scattering from individual particles does not produce NP in this range. The real part Re(m) plays little role in this case. We confirm the particle size effect for NP at high packing density predicted by approximate models and laboratory measurements for absorbing samples. We also demonstrate that NP is a result of an interplay between single- and multiple scattering in a medium. This balance can be controlled by the topology of a monolayer resulting in enhanced or damped NP. We show also that re-orienting particles targeted to reduced double scattering may turn NP off even at maximum packing density. These factors should be taken into account when analyzing the photopolarimetric data obtained for low-albedo objects.

Acknowledgments

The authors gratefully acknowledge the computing time support provided by the Paderborn Center for Parallel Computing (PC^2).

References

[1] Y. Shkuratov, G. Videen, M. Kreslavsky, I. Belskaya, V. Kaydash, A. Ovcharenko, V. Omelchenko, N. Opanasenko, E. Zubko, Scattering properties of planetary regoliths near opposition, in: G. Videen, Y. Yatskiv, M. Mishchenko (Eds.), Photopolarimetry in remote sensing, Springer, 2004, pp. 191–208.

[2] M. I. Mishchenko, V. Rosenbush, N. Kiselev, D. Lupishko, V. Tishkovets, V. Kaydash, I. Belskaya, Y. S. Efimov, N. Shakhovskoy, Polarimetric remote sensing of solar system objects, Akademperiodyka, 2010.

[3] Y. Shkuratov, A. Ovcharenko, E. Zubko, O. Miloslavskaya, K. Muinonen, J. Piironen, R. Nelson, W. Smythe, V. Rosenbush, P. Helfenstein, The opposition effect and negative polarization of structural analogs for planetary regoliths, Icarus 159 (2) (2002) 396–416.

[4] H. Palme, K. Lodders, A. Jones, Solar system abundances of the elements, Planets, Asteriods, Comets and The Solar System, Volume 2 of Treatise on Geochemistry (Second Edition). Edited by Andrew M. Davis. Elsevier, 2014., p.15-36 2 (2014). doi:10.1016/B978-0-08-095975-7.00118-2.
URL https://par.nsf.gov/biblio/10036398

[5] A. Mahjoub, M. E. Brown, M. J. Poston, R. Hodyss, B. L. Ehlmann, J. Blacksberg, M. Choukroun, J. M. Eiler, K. P. Hand, Effect of h2s on the near-infrared spectrum of irradiation residue and applications to the kuiper belt object (486958) arrokoth, The Astrophysical Journal Letters 914 (2) (2021) L31. doi:10.3847/2041-8213/ac044b.
URL https://dx.doi.org/10.3847/2041-8213/ac044b

[6] M. J. Loeffler, P. D. Tribbett, J. F. Cooper, S. J. Sturner, A possible explanation for the presence of crystalline h2o-ice on kuiper belt objects, Icarus 351 (2020) 113943.

[7] W. D. Carrier, , Journal of Geotechnical and Geoenvironmental Engineering 129 (10) (2003) 956–959.

[8] A. Kokhanovsky, G. de Leeuw (Eds.), Light scattering by large densely packed clusters of particles, Praxis, Chichester, UK, 2009.

[9] L. Kolokolova, J. Hough, A. Levasseur-Regourd (Eds.), Polarimetry of Stars and Planetary Systems, Cambridge University Press, 2015.

[10] I. Belskaya, A. Cellino, A.-C. Levasseur-Regourd, S. Bagnulo, Optical polarimetry of small solar system bodies: From asteroids to debris disks,

in: R. Mignani, A. Shearer, A. Słowikowska, S. Zane (Eds.), Astronomical Polarisation from the Infrared to Gamma Rays, Springer International Publishing, Cham, 2019, pp. 223–246.

[11] L. Sun, P. G. Lucey, C. I. Honniball, M. Sandford, E. S. Costello, L. Burkhard, R. Brennan, C. Ferrari-Wong, Hyperspectral polarimetry of eight apollo soils, Icarus 372 (2022) 114740. doi:https://doi.org/10.1016/j.icarus.2021.114740.
URL https://www.sciencedirect.com/science/article/pii/S0019103521003936

[12] A.-C. Levasseur-Regourd, J.-B. Renard, Y. Shkuratov, E. Hadamcik, Laboratory studies, in: L. Kolokolova, J. Hough, A.-C. Levasseur-Regourd (Eds.), Polarimetry of Stars and Planetary Systems, Cambridge University Press, 2015, pp. 62–80.

[13] A. A. Ovcharenko, S. Y. Bondarenko, E. S. Zubko, Y. G. Shkuratov, G. Videen, R. M. Nelson, W. D. Smythe, Particle size effect on the opposition spike and negative polarization, Journal of Quantitative Spectroscopy and Radiative Transfer 101 (3) (2006) 394–403.

[14] K. Muinonen, A. Penttilä, G. Videen, Multiple scattering of light in particulate planetary media, in: L. Kolokolova, J. Hough, A.-C. Levasseur-Regourd (Eds.), Polarimetry of Stars and Planetary Systems, Cambridge University Press, 2015, pp. 114–129.

[15] Y. Shkuratov, M. Kreslavsky, A. Ovcharenko, D. Stankevich, E. Zubko, C. Pieters, G. Arnold, Opposition effect from clementine data and mechanisms of backscatter, Icarus 141 (1) (1999) 132–155. doi:https://doi.org/10.1006/icar.1999.6154.
URL https://www.sciencedirect.com/science/article/pii/S0019103599961547

[16] M. Kaveh, M. Rosenbluh, I. Edrei, I. Freund, Weak localization and light scattering from disordered solids, Phys. Rev. Lett. 57 (1986) 2049–2052. doi:10.1103/PhysRevLett.57.2049.
URL https://link.aps.org/doi/10.1103/PhysRevLett.57.2049

[17] K. Muinonen, Electromagnetic scattering by two interacting dipoles, Proc. 1989 URS1 Electromagnetic Theory Sympos., Stockholm, Sweden (1989) 428–430.

[18] Y. Shkuratov, On the opposition brightness surge and light negative polarization of solid cosmic surfaces, Astronomicheskii Tsirkulyar 1400 (1985) 3–6, in Russian.

[19] Y. Shkuratov, Interference mechanism of opposition spike and negative polarization of atmosphereless planetary bodies, Bulletin of the American Astronomical Society 21 (1989) 989.

[20] Y. Grynko, Y. Shkuratov, J. Förstner, Light backscattering from large clusters of densely packed irregular particles, Journal of Quantitative Spectroscopy and Radiative Transfer 255 (2020) 107234.

[21] Y. Grynko, Y. Shkuratov, S. Alhaddad, J. Förstner, Negative polarization of light at backscattering from a numerical analog of planetary regoliths, Icarus 384 (2022) 115099.

[22] S. Alhaddad, Y. Grynko, H. Farheen, J. Förstner, Numerical analysis of the coherent mechanism producing negative polarization at backscattering from systems of absorbing particles, Opt. Lett. 47 (1) (2022) 58–61.

[23] Y. Shkuratov, S. Bondarenko, A. Ovcharenko, C. Pieters, T. Hiroi, H. Volten, O. Muñoz, G. Videen, Comparative studies of the reflectance and degree of linear polarization of particulate surfaces and independently scattering particles, Journal of Quantitative Spectroscopy and Radiative Transfer 100 (1) (2006) 340–358.

[24] Y. Grynko, Y. Shkuratov, J. Förstner, Intensity surge and negative polarization of light from compact irregular particles, Opt. Lett. 43 (15) (2018) 3562–3565.

[25] Y. Grynko, Y. Shkuratov, J. Förstner, Light backscattering from large clusters of densely packed irregular particles, Journal of Quantitative Spectroscopy and Radiative Transfer 255 (2020) 107234.

[26] G. Videen, Polarization opposition effect and second-order ray tracing, Appl. Opt. 41 (24) (2002) 5115–5121.

[27] Y. Grynko, Y. Shkuratov, S. Alhaddad, J. Förstner, Light scattering by large densely packed clusters of particles, in: A. Kokhanovsky (Ed.), Springer Series in Light Scattering: Volume 8: Light Polarization and

Multiple Scattering in Turbid Media, Springer International Publishing, 2022, in press.

[28] A. V. Konoshonkin, N. V. Kustova, A. G. Borovoi, Y. Grynko, J. Förstner, Light scattering by ice crystals of cirrus clouds: comparison of the physical optics methods, Journal of Quantitative Spectroscopy and Radiative Transfer 182 (2016) 12–23.

[29] T. Väisänen, J. Markkanen, E. Hadamcik, J.-B. Renard, J. Lasue, A. C. Levasseur-Regourd, J. Blum, K. Muinonen, Scattering of light by a large, densely packed agglomerate of small silica spheres, Opt. Lett. 45 (7) (2020) 1679–1682.

[30] J. S. Hesthaven, T. Warburton, Nodal high-order methods on unstructured grids: I. time-domain solution of maxwell's equations, Journal of Computational Physics 181 (1) (2002) 186–221.

[31] E. Grin'ko, Y. G. Shkuratov, The scattering matrix of transparent particles of random shape in the geometrical optics approximation, Optics and Spectroscopy 93 (6) (2002) 885–893.

[32] Y. G. Shkuratov, Y. S. Grynko, Light scattering by media composed of semitransparent particles of different shapes in ray optics approximation: consequences for spectroscopy, photometry, and polarimetry of planetary regoliths, Icarus 173 (1) (2005) 16–28.

[33] B. W. Hapke, On the particle size distribution of lunar soil, Planetary and Space Science 16 (1) (1968) 101–110. doi:https://doi.org/10.1016/0032-0633(68)90047-0.
URL https://www.sciencedirect.com/science/article/pii/0032063368900470

[34] E. Coumans, Y. Bai, Pybullet, a python module for physics simulation for games, robotics and machine learning, http://pybullet.org (2016–2021).

[35] W. W. Duley, Identification of some diffuse interstellar features, Astrophysics and Space Science 88 (2) (1982) 501–505. doi:10.1007/BF01092716.
URL https://doi.org/10.1007/BF01092716

[36] W. H. Dalzell, A. F. Sarofim, Optical Constants of Soot and Their Application to Heat-Flux Calculations, Journal of Heat Transfer 91 (1) (1969) 100–104. arXiv:https://asmedigitalcollection.asme.org/heattransfer/article-pdf/91/1/100/5751373/100_1.pdf, doi:10.1115/1.3580063.
URL https://doi.org/10.1115/1.3580063

[37] E. S. Zubko, A. A. Ovcharenko, Y. G. Shkuratov, Polarimetric weak-localization effect in scattering of natural light in the region of small phase angles, Optics and Spectroscopy 92 (3) (2002) 443–448. doi:10.1134/1.1465472.
URL https://doi.org/10.1134/1.1465472

[38] M. I. Mishchenko, L. Liu, J. W. Hovenier, Effects of absorption on multiple scattering by random particulate media: exact results, Opt. Express 15 (20) (2007) 13182–13187. doi:10.1364/OE.15.013182.
URL https://opg.optica.org/oe/abstract.cfm?URI=oe-15-20-13182

[39] E. Zubko, Y. Shkuratov, M. Mishchenko, G. Videen, Light scattering in a finite multi-particle system, Journal of Quantitative Spectroscopy and Radiative Transfer 109 (12) (2008) 2195–2206. doi:https://doi.org/10.1016/j.jqsrt.2008.03.007.
URL https://www.sciencedirect.com/science/article/pii/S0022407308000733

[40] P.-W. Zhai, Y.-K. Lee, G. W. Kattawar, P. Yang, Implementing the near- to far-field transformation in the finite-difference time-domain method, Appl. Opt. 43 (18) (2004) 3738–3746. doi:10.1364/AO.43.003738.
URL https://opg.optica.org/ao/abstract.cfm?URI=ao-43-18-3738

[41] M. S. Hanner, R. H. Giese, K. Weiss, R. Zerull, On the definition of albedo and application to irregular particles, Astronomy and Astrophysics 104 (1) (1981) 42–46.